Bull. Mater. Sci., Vol. 31, No. 7, December 2008, pp. 987–993. © Indian Academy of Sciences.

Metathesis synthesis and characterization of complex metal fluoride, KMF_3 (M = Mg, Zn, Mn, Ni, Cu and Co) using mechanochemical activation

V MANIVANNAN*, P PARHI and JONATHAN W KRAMER

Department of Mechanical Engineering, Campus Delivery 1374, Colorado State University, Fort Collins, CO 80523, USA

MS received 30 April 2008

Abstract. **Metathesis synthesis of complex metal fluorides using mechanochemical activation has been reported. The high lattice energy of the byproduct KCl helps the reaction towards product formation in under 20 min. The proposed process, in contrast to the available methods of synthesis, is very rapid, economical and results in products with controlled morphology. The structural, optical and chemical properties of synthesized powders are determined by powder X-ray diffraction, scanning electron microscopy, X-ray photoelectron spectroscopy, magnetization measurements and diffused reflectance spectra in the UV–VIS range.**

Keywords. **Perovskites; KMF_3; structure–property relations.**

1. Introduction

Complex perovskites fluorides show various important properties such as piezoelectric characteristics, ferromagnetic, non-magnetic insulator behaviour and photoluminescence (Cooke *et al* 1975; Alcala *et al* 1982; Heaton and Lin 1982; Mortier *et al* 1994; Tan and Shi 2000). It is well known that these complex fluorides can be prepared by conventional solid state reaction (Somiya *et al* 1981; Dzik *et al* 2000), microemulsion method (Cao *et al* 2004; Hua *et al* 2007), and hydrothermal technique (Zhao *et al* 1996; Li *et al* 2000). All these synthetic routes need either expensive equipment or high temperature. Low temperature hydrothermal synthesis is the next alternative method for the synthesis, but in this synthetic process it is difficult to control the reaction kinetics (Sreeja and Joy 2007). Mechanochemical synthesis of inorganic oxides is an alternative to the solid state high temperature synthesis and soft synthetic route. Mechanochemical synthesis assisted by ball milling has been successfully used in the past for the synthesis of nanoparticles of oxides and fluorides (Lee *et al* 2001). The main advantage of the mechanical synthesis is that it provides intense energy in localized parts of the reactive precursors where solid state diffusion and dissolution are forced on, even though the resulting material may be thermodynamically unstable. Applying such a procedure, Lee *et al* synthesized complex metal fluorides with perovskite structures (Lee *et al* 2001, 2003). They have milled the metal fluorides along with potassium fluorides for 6 h to form KMF_3 (M = Mg, Ca, Zn, Mn, Ni and Co) followed by annealing at 673 K for 2 h to confirm the single-phase formation.

Further procedural simplification for the synthesis of the technologically important fluorides is desired, and we report the successful synthesis of such fluorides by solid-state metathesis (SSM) approach. Metathesis-type reactions ($2CaCl_2 + Na_2WO_4 \rightarrow 2CaWO_4 + 2NaCl$, as an example) are fast, self-energetic reactions which involve the exchange of reacting partners, and are largely driven by the high lattice energy of byproducts like NaCl (removed by washing) (Panda *et al* 2003). SSM reactions are well reported in the literature for the synthesis of metal pnictides (Treece *et al* 1994), chalcogenides (Bonneau *et al* 1991), carbides (Nartowski *et al* 1999), silicides (Fitzmaurice *et al* 1995), and borides (Rao *et al* 1995). For example, Gopalakrishnan and his coworkers have synthesized various metal oxides (both binary and ternary) and perovskite materials using this metathesis approach (Gopalakrishnan *et al* 1997, 2000; Sivakumar and Gopalakrishnan 2002; Sivakumar *et al* 2004; Mandal and Gopalakrishnan 2005). Although metathesis reactions may initiate spontaneously, most are typically initiated by providing additional energy to overcome the small energy barrier which helps in spontaneous reaction. Ramanan and his coworkers have synthesized biologically active phosphates by microwave mediated metathesis synthesis (Parhi *et al* 2004, 2006a,b 2007). We have recently demonstrated the versatility of the approach by synthesizing several materials with commercial applications (Manivannan *et al* 2008).

*Author for correspondence (mani@engr.colostate.edu)

The objective of this work is to apply an established SSM approach initiated by high-energy ball milling (mechanochemical synthesis) and demonstrate the feasibility to synthesize technologically important KMF_3 type fluorides in relatively short period of time. The proposed method has the advantage of producing nanosized particles with controlled morphology in addition to simplicity. Mechanochemical synthesis assisted by an SSM approach to synthesize complex fluorides of the type, KMF_3 (M = Mg, Ca, Zn, Mn, Ni and Co) has not been reported so far.

2. Experimental

KF, $ZnCl_2$, $MnCl_2{\cdot}4H_2O$, $NiCl_2{\cdot}6H_2O$, $CuCl_2$, $MgCl_2{\cdot}6H_2O$ and $CoCl_2{\cdot}6H_2O$ starting materials were obtained from Alfa Aesar, USA, and used as received. For the synthesis of ternary metal fluorides, KF and $MCl_2{\cdot}xH_2O$ (M = Mg, Zn, Mn, Ni, Cu and Co) were added in a 3 : 1 molar ratio and grinded using SPEX 8000 Mixer Mill for a maximum period of 20 min. The resultant powders were washed with water and dried with ethanol at 90°C overnight to get the desired product.

Powder X-ray diffraction (XRD) measurements were carried out with Scintag X2 diffractometer with CuK_α radiation. A scan rate of 1 degree/min with a step size of 0·02° was employed to obtain the XRD spectra. Search match analysis was performed using Bruker EVA software. Scanning electron microscopy (SEM) characterization equipped with energy dispersive X-ray analysis (EDX) was performed on the JSM-6500F, a field emission system with the in-lens thermal field emission electron gun. Diffuse reflectance (DR) spectra was recorded in the wavelength range 250–2500 nm using Varian Associates 500 double beam spectrophotometer equipped with Praying mantis.

Compressed polytetrafluoroethylene was used for standard calibration (100% reflectance). X-ray photoelectron spectroscopy (XPS) experiments were performed on a Physical Electronics 5800 spectrometer. This system has a monochromatic Al K_α X-ray source (h_α = 1486·6 eV), hemispherical analyser, and multichannel detector. A low energy (30 eV) electron gun was used for charge neutralization on the non-conducting samples. Magnetic measurements were taken using a Quantum Design 5·0 Tesla Magnetic Properties Measurement System (MPMS–XL). The system can operate at temperatures from 1·8 to 400 K. All the samples were subjected to an applied magnetic field of 1000 Gauss.

3. Results and discussion

Figure 1 shows XRD of $KZnF_3$ and $KMnF_3$ phases synthesized by this mechanochemical process. Figure 1a shows the XRD pattern of the synthesized solid before washing, where KCl (peaks marked with *) and the desired product phase are present together. The presence of KCl in the unwashed product strongly indicates that the reaction

$$ZnCl_2 + 3KF \rightarrow KZnF_3 + 2KCl, \quad (1)$$

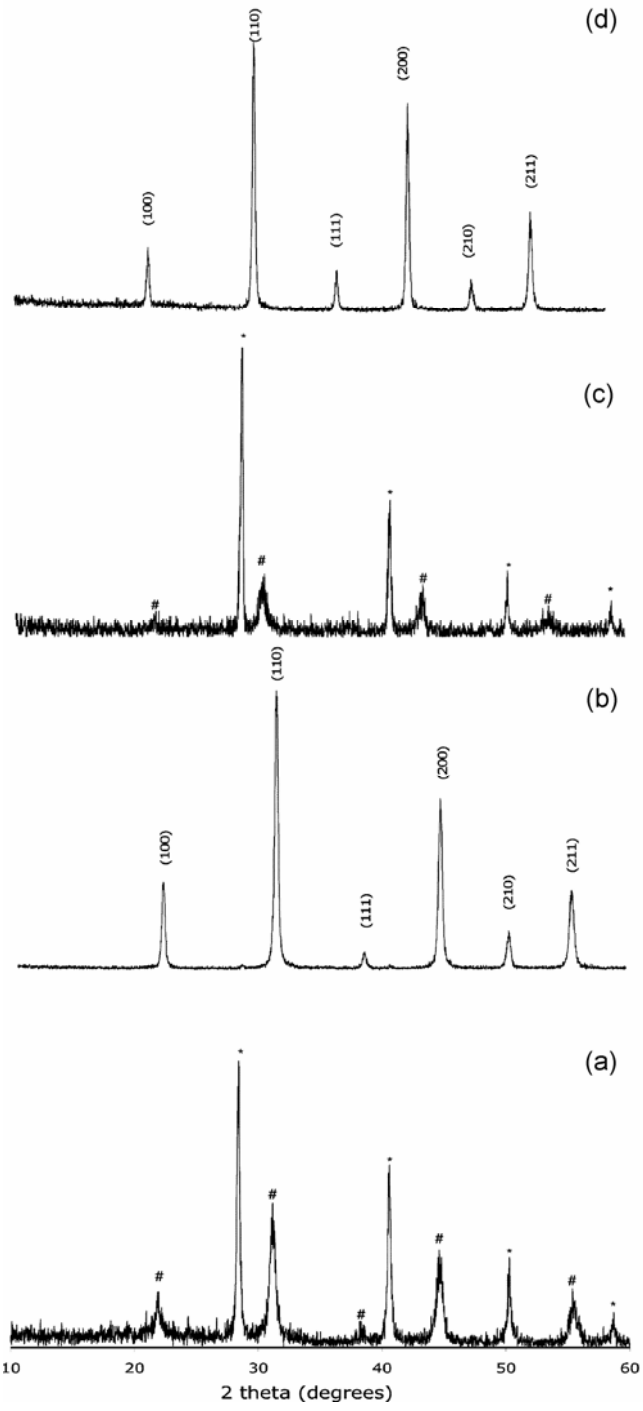

Figure 1. Powder X-ray diffraction patterns of (a) as-prepared sample of $KZnF_3$, (b) single-phase $KZnF_3$ after washing off the KCl byproduct, (c) as-prepared sample of $KMnF_3$, and (d) single-phase $KMnF_3$ after washing off the KCl byproduct. * corresponds to the KCl phase and # corresponds to the synthesized fluoride phase.

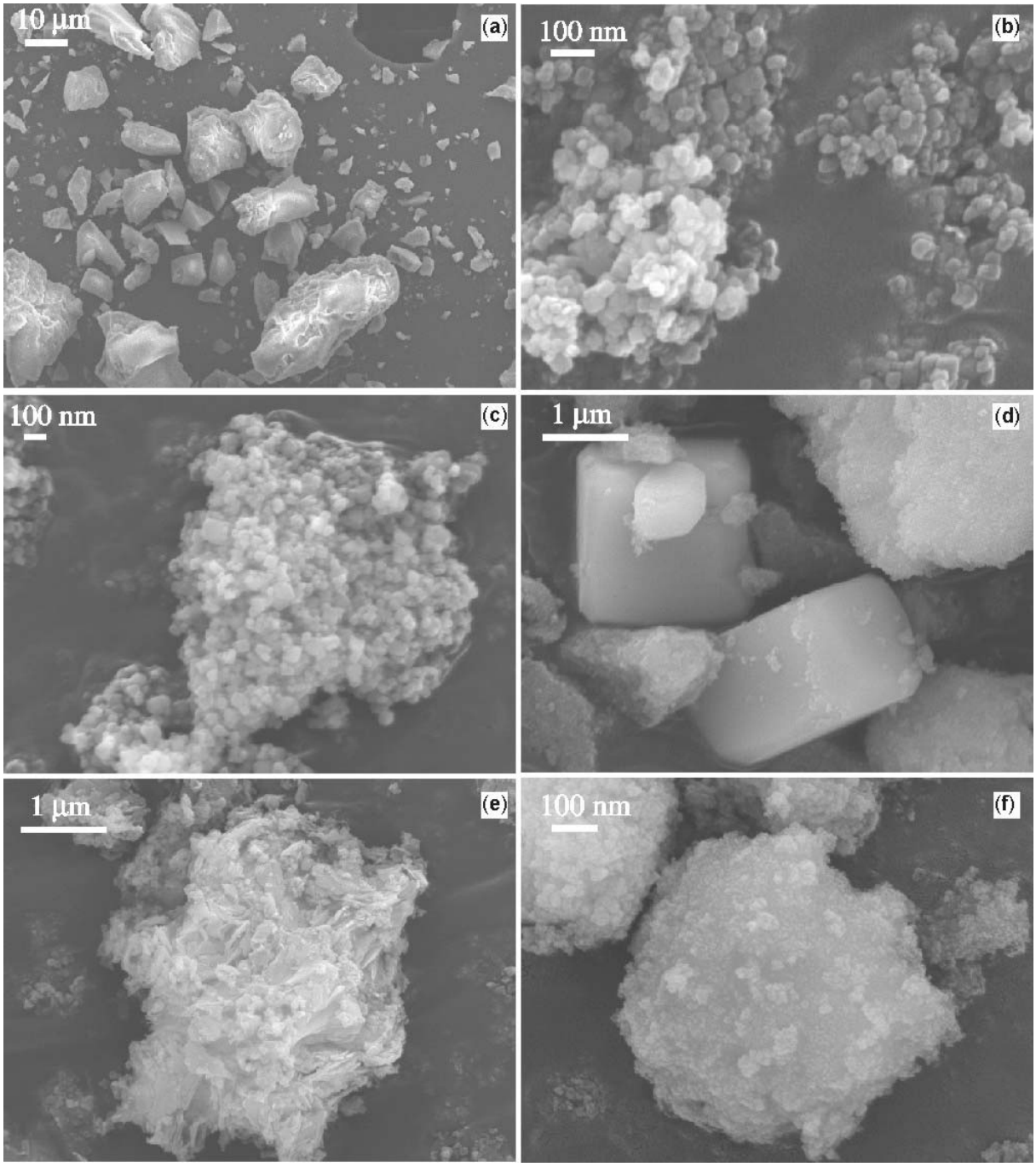

Figure 2. SEM images of (**a**) $KMgF_3$, (**b**) $KZnF_3$, (**c**) $KMnF_3$, (**d**) $KNiF_3$, (**e**) $KCuF_3$, and (**f**) $KCoF_3$ synthesized by ball milling.

occurred in a metathetic pathway. Figure 1b shows XRD of single phase $KZnF_3$ after washing off the KCl byproduct. Figure 1c shows XRD pattern of the synthesized solids before washing, where KCl peaks are marked with *. The presence of KCl in the unwashed product strongly indicates that the reaction

$$MnCl_2{\cdot}4H_2O + 3KF \rightarrow KMnF_3 + 2KCl + 4H_2O, \quad (2)$$

occurred in a metathetic pathway. Figure 1d shows XRD of single phase $KMnF_3$ after washing off the KCl byproduct.

Samples of $KMgF_3$, $KNiF_3$, $KCuF_3$ and $KCoF_3$ were synthesized as described above. In all cases the presence of KCl (per XRD) in the before washed samples signifies the metathetic nature of the reaction. XRD analysis showed the desired product formation in comparison with a JCPDS standard (JCPDS cards) and accordingly the patterns were indexed. Among perovskite KMF_3 type fluorides (M = Mg, Ni, Cu, Co) synthesized, except for Mg compound, some impurity peaks were noticed in other fluorides. Peak broadening of the XRD patterns suggested

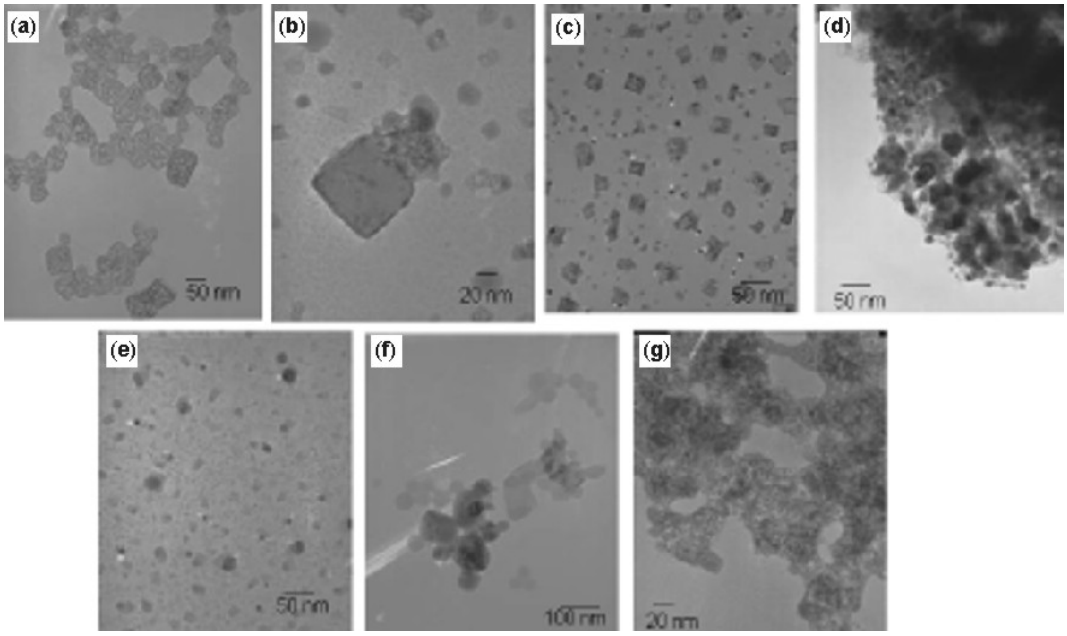

Figure 3. TEM images of (**a**) and (**b**) $KZnF_3$, (**c**) $KNiF_3$, (**d**) $KZnF_3$, (**e**) and (**f**) $KCuF_3$ and (**g**) $KCoF_3$ synthesized by ball milling.

Table 1. Crystal structure details of KMF_3 (M = Mg, Zn, Mn, Ni, Co and Cu).

	a(Å)	*c*(Å)	*V* (Å^3)	*Z*	Space group
$KMgF_3$	3·988(9)		63·47	1	*Pm3m*
$KZnF_3$	4·055(0)		66·68	1	*Pm3m*
$KMnF_3$	4·182(0)		73·14	1	*Pm3m*
$KNiF_3$	4·012(7)		64·61	1	*Pm3m*
$KCoF_3$	4·070(8)		67·46	1	*Pm3m*
$KCuF_3$	5·855(0)	7·852(0)	269·17	4	*Pm3m*

a possible nano-size particle nature of the materials synthesized by this method. Table 1 summarizes the crystal structure details of all the fluorides synthesized in this study.

Figure 2 shows the SEM images of the synthesized fluorides. Figures 2a–f show SEM images of $KMgF_3$, $KZnF_3$, $KMnF_3$, $KNiF_3$, $KCuF_3$ and $KCoF_3$, respectively. $KZnF_3$, $KMnF_3$ and $KNiF_3$ materials showed cubic morphology as per SEM. Nano-sized particles can be synthesized in case of $KZnF_3$, $KMnF_3$ and $KCoF_3$. SEM also showed that the particles are agglomerated in most of the cases. EDX patterns of these fluorides are consistent with the chemical compositions and stoichiometry of the materials. To confirm the nanoparticle features, TEM was performed on the fluoride samples (figure 3), which revealed the particles are indeed nano-sized (~ 20 nm). TEM also showed that the particles exhibited well defined cubic morphologies.

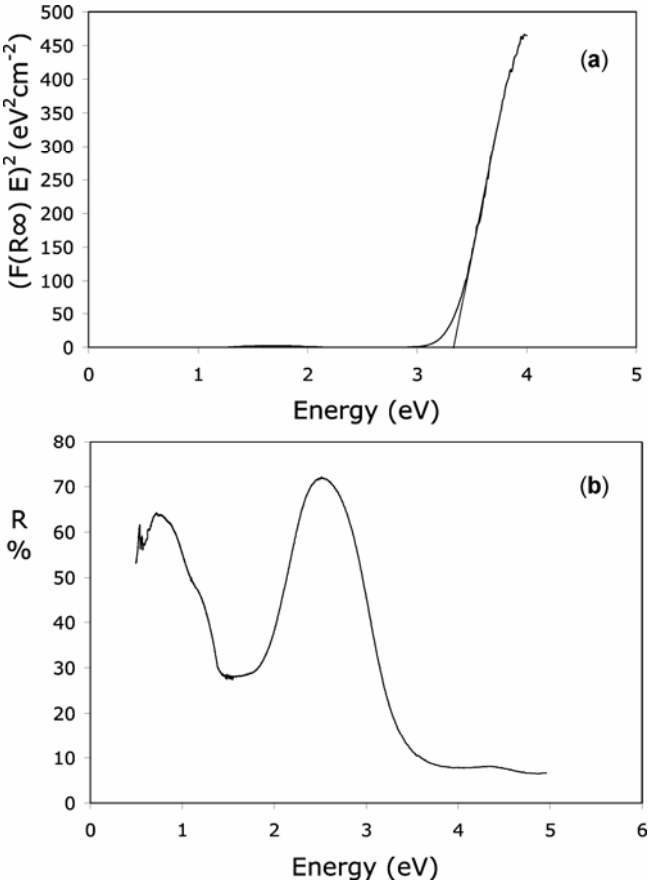

Figure 4. (**a**) Diffuse reflectance spectra of $KCuF_3$ in the wavelength range 250–2500 nm and (**b**) plot of $F(R_\infty)$ vs E (eV) for the estimation of the optical absorption edge energy.

XPS analysis was performed to examine the composition of the synthesized fluorides. In the full spectrum analysis of $KZnF_3$ (not shown), a very weak O 1*s* peak at 531·3 eV can be ascribed to the absorbed water on the surface of the fluorides which is consistent with EDX analysis. Also, a small adsorbed carbon C1*s* peak positioned at 284·5 eV was used to calibrate the acquired spectrum. The spectrum and the position of F1*s* (684·3eV), K2*p* (292·2 eV), and Zn $2p_{3/2}$ (~1022·7 eV) agree with those reported for ZnF_2 and KF (Chastain 1992; Li *et al* 2000).

In semiconductor technological applications, vacuum-ultraviolet transparent (VUT) materials for lenses in optical lithography are needed (Sahnoun *et al* 2005). KMF_3 materials with perovskite structures are potential candidates and received recent attention because they do not have birefringence, which makes design of lenses difficult. The suitability of these materials is largely dependent on the electronic properties, which are affected by the band-gap of the material (E_g). To determine the E_g, we have performed the diffuse reflectance spectra of some of the KMF_3 (M = Cu, Co) samples in the UV–VIS–NIR range.

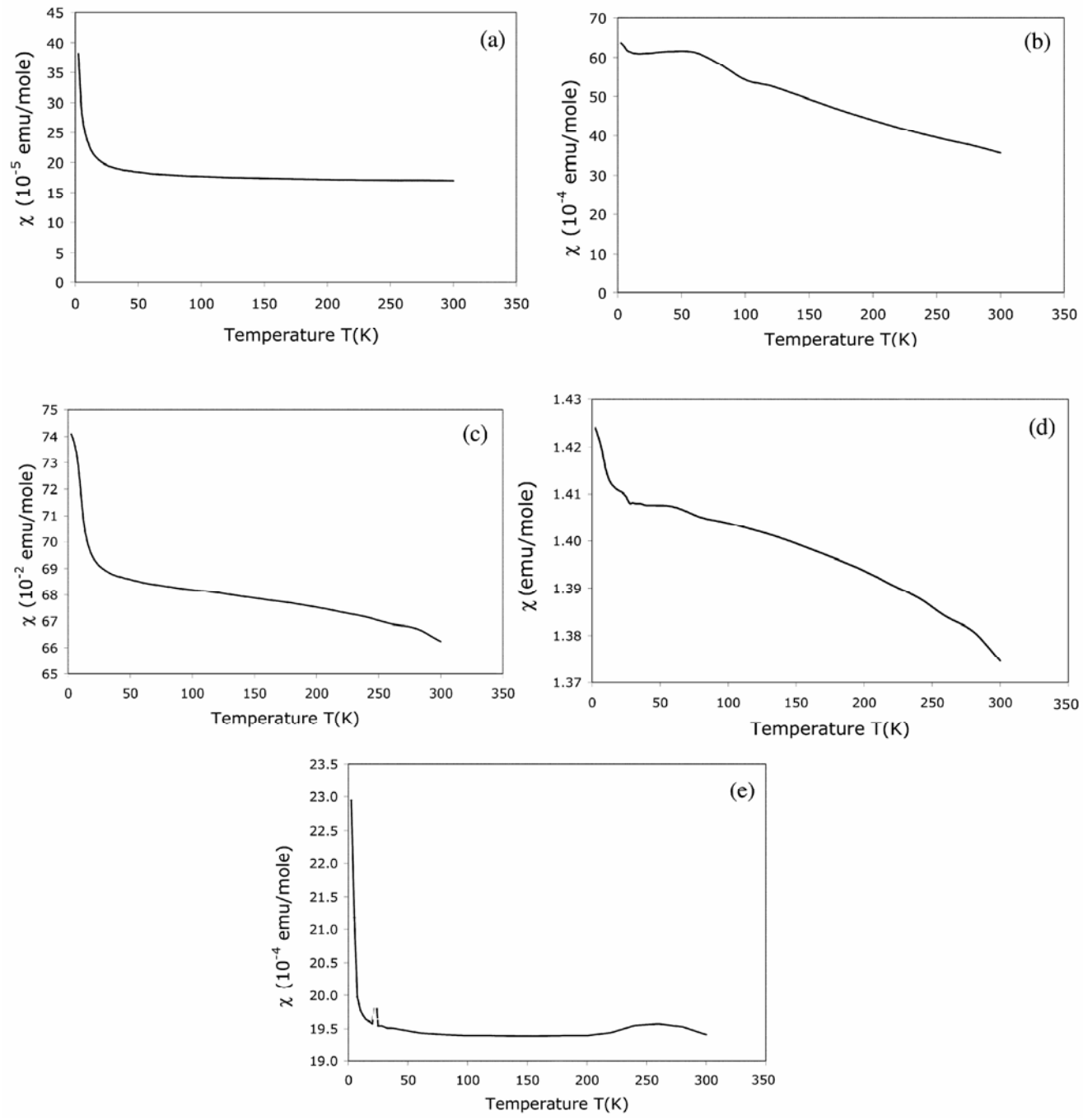

Figure 5. Magnetization of (**a**) $KZnF_3$, (**b**) $KMnF_3$, (**c**) $KNiF_3$, (**d**) $KCoF_3$ and (**e**) $KCuF_3$.

Figure 4 shows the diffuse reflectance spectra of the $KCuF_3$ sample in the UV–VIS–NIR range. The diffuse reflectance data of figure 4a was used to calculate the absorption coefficient from the Kubelka–Munk (KM) function (Kortum 1969) defined as:

$$F(R_\infty) = \frac{\alpha}{S} = \frac{(1-R_\infty)^2}{2R_\infty},$$

where

$$R_\infty = \frac{R_{\text{sample}}}{R_{\text{PTFE}}}.$$

Here α is the absorption coefficient, S the scattering coefficient, and $F(R_\infty)$ the KM function. The energy dependence of the material in the UV–VIS–NIR was further explored. The energy dependence of semiconductors near the absorption edge is expressed as

$$\alpha E = K(E - E_g)^\eta.$$

Here E is the incident photon energy ($h\nu$), E_g the optical absorption edge energy, K a constant and exponent η is dependent on the type of optical transition as a result of photon absorption (Barton *et al* 1999). The η is assigned a value of 1/2, 3/2, 2 and 3 for direct allowed, direct forbidden, indirect allowed, and indirect forbidden transitions, respectively (Tauc *et al* 1966). For the diffused reflectance spectra, the KM function can be used instead of α for estimation of the optical absorption edge energy (Barton *et al* 1999). It was observed that a plot of $F(R_\infty)E$ vs E was linear near the edge for direct allowed transition ($\eta = 1/2$). The intercept of the line on the abscissa ($F(R_\infty)E = 0$) gave the value of optical absorption edge energy as $3{\cdot}3 \pm 0{\cdot}2$ eV (figure 4b) for $KCuF_3$. Similarly, the bandgap for $KCoF_3$ was determined to be $2{\cdot}1 \pm 0{\cdot}2$ eV for $KCoF_3$. The E_g determined (for $KCoF_3$) is in agreement with the E_g predicted (2·4) from modeling studies using the local spin density approximation approach (Punkkinen 1999). The results indicate $KCoF_3$ and $KCuF_3$ materials are likely to be insulators, the size of their energy gap is determined by increased charge transfer energy caused by the more ionic nature of M–F bonding (M = Mg, Zn, Mn, Ni, Cu and Co), and accordingly these materials have the potential to be used for optical materials for UV/VUV regions. The diffused reflectance spectra for direct bandgap orthorhombic (β) Ta_2O_5 (Sahu and Kleinman 2004) prepared by heating Ta metal in air is also recorded for comparison. The value of optical absorption edge energy for indirect allowed transition for Ta_2O_5 was found to be $4 \pm 0{\cdot}2$ eV, which is consistent with those seen for the β-Ta_2O_5 reported earlier (Knausenberger and Tauber 1973).

3.1 *Magnetic properties*

The magnetic properties of KMF_3 materials in relation to their perovskite crystal structures have been investigated (Knox 1961; Machin *et al* 1963; Pari *et al* 1994) and shown in figure 5. The KMF_3 compounds are antiferromagnetic, the Neel points being ~85 K ($KNiF_3$, figure 5b), ~275 K ($KNiF_3$, figure 5c), ~80 K ($KCoF_3$, figure 5d), and ~240 K ($KCuF_3$, figure 5e), all of which matches closely with the reported values (Hirakawa *et al* 1960). The increase in the Neel points in the sequence Co < Ni is consistent with the ionic radii of the transition metals which decrease in the same order (Machin *et al* 1963). $KZnF_3$ compounds showed paramagnetic behaviour from room-temperature down to 4 K (figure 5a).

4. Conclusions

Mechanochemical synthesis has been successfully employed for the synthesis of complex metal fluorides of the type, KMF_3. The proposed method is simple, less labour intensive, and less time consuming. The products were characterized for structural, chemical and optical properties. The optical transition bandgap of the $KCuF_3$ and $KCoF_3$ were determined to be $3{\cdot}3 \pm 0{\cdot}2$ eV and $2{\cdot}1 \pm 0{\cdot}2$ eV, respectively.

Acknowledgements

The authors would like to acknowledge Prof. Allan Kirkpatrick, Department Head, Mechanical Engineering, Colorado State University, for his continued help, encouragement and support.

References

Alcala R, Sardar D K and Sibley W A 1982 *J. Luminesc.* **27** 273

Barton D G, Shtein M, Wilson R D, Soled S L and Iglesia E 1999 *J. Phys. Chem.* **B103** 630

Bonneau P R, Jarvis R F and Kaner R B 1991 *Nature* **349** 510

Cao M, Wang Y, Qi Y, Guo C and Hu C 2004 *J. Solid State Chem.* **177** 2205

Chastain J 1992 *Handbook of X-ray photoelectron spectroscopy* (MN, USA: Perkin, Eden Prairie)

Cooke A H, Jones D A, Silva J F A and Weils M R 1975 *J. Phys. C: Solid State Phys.* **8** 4083

Dzik G D, Sokolska I, Golab S and Baluka M 2000 *J. Alloys and Compds* **300** 254

Fitzmaurice J C, Hector A L, Parkin I P and Rowley A T 1995 *Phosphorus sulfur silicon and related elements* **101** 47

Kortum G 1969 *Reflectance spectroscopy principles, methods, applications* (New York: Springer-Verlag)

Gopalakrishnan J, Pandey S and Kasturi Rangan K 1997 *Chem. Mater.* **9** 2113

Gopalakrishnan J, Sivakumar T, Ramesha K, Thangadurai V and Subbanna G N 2000 *J. Am. Chem. Soc.* **122** 6237

Heaton R A and Lin C C 1982 *Phys. Rev.* **B25** 3538

Hirakawa K, Hirakawa K and Hashimoto T 1960 *J. Phys. Soc. Jap.* **15** 2063

Hua R, Jia Z and Shi C 2007 *Mater. Res. Bull.* **42** 249

JCPDS-International Centre for Diffraction Data 2000 JCPDS Card Nos 18-1006, 18-1033, 72-113, 72-109, 21-1002, 72-1473, ICDD, PCPDFWIN v.2.1

Knausenberger W H and Tauber R N 1973 *J. Electrochem. Soc.* **129** 927

Knox K 1961 *Acta Crystallogr.* **14** 583

Lee J, Zhang Q and Saito F 2001 *Chem. Lett.* **7** 700

Lee J, Shin H, Lee J, Chung H, Zhang Q and Saito F 2003 *Mater. Trans.* **44** 1457

Li H, Jia Z and Shi C 2000 *Chem. Lett.* **9** 1106

Mandal T K and Gopalakrishnan J 2005 *Chem. Mater.* **17** 2310

Machin D D, Martin R L and Nyholm R S 1963 *J. Chem. Soc.* **44** 1490

Manivannan V, Parhi P and Howard J 2008 *J. Cryst. Growth* **310** 2793

Mortier M, Gesland J Y and Rousseau M 1994 *Solid State Commun.* **89** 369

Nartowski A M, Parkin I P, Mackenzie M, Craven A J and Macleod I 1999 *J. Mater. Chem.* **9** 1275

Panda M, Seshadri R and Gopalakrishnan J 2003 *Chem. Mater.* **15** 1554

Parhi P, Ramanan A and Ray A R 2004 *Mater. Lett.* **58** 3610

Parhi P, Ramanan A and Ray A R 2006a *Mater. Lett.* **60** 218

Parhi P, Ray A R and Ramanan A R 2006b *Am. J. Biochem. and Biotech.* **2** 61

Parhi P, Ray A R and Ramanan A R 2007 *J. Am. Ceram. Soc.* **90** 1237

Pari G, Mathi Jaya S and Asokamani R 1994 *Phys. Rev.* **B50** 8166

Punkkinen M P J 1999 *Solid State Commun.* **11** 477

Rao L, Gillan E G and Kaner R B 1995 *J. Mater. Res.* **10** 353

Sahnoun M, Zbiri M, Daul C, Jhenata R, Baltache H and Driz M 2005 *Mater. Chem. and Phys.* **91** 185

Sahu B R and Kleinman L 2004 *Phys. Rev.* **B69** 165202/1

Sivakumar T and Gopalakrishnan J 2002 *Chem. Mater.* **14** 3984

Sivakumar T, Lofland S E, Ramanujachary K V, Ramesha K, Subbanna G N and Gopalakrishnan J 2004 *J. Solid State Chem.* **177** 2635

Somiya S, Hirano S, Yoshimura M and Yanagisawa K 1981 *J. Mater. Sci.* **16** 813

Sreeja V and Joy P A 2007 *Mater. Res. Bull.* **42** 1570

Tan Y and Shi C 2000 *J. Solid State Chem.* **150** 178

Tauc J, Grigorov R and Vancu A 1966 *Phys. Status Solidi* **15** 627

Treece R E, Conklin J A and Kaner R B 1994 *Inorg. Chem.* **33** 5701

Zhao C, Feng S, Chao Z, Shi C, Xu R and Ni J 1996 *Chem. Commun.* **14** 1641